

Modeling Reservation-based Autonomous Intersection Control in VISSIM

A Paper Submitted to
the Transportation Research Board
for Review for Presentation & Publication
at the TRB 92nd Annual Meeting in Washington, D.C., January 13-17, 2013

Zhixia Li, Ph.D.
Research Associate
1249A Engineering Hall, 1415 Engineering Drive, Madison WI 53706
Phone: 513-484-2991; Fax: (608)262-5199
Email: zli262@wisc.edu

Madhav V. Chitturi, Ph.D.
Assistant Researcher
B243 Engineering Hall, 1415 Engineering Drive, Madison, WI 53706
Phone: (608)890-2439, Fax: (608)262-5199
Email: mchitturi@wisc.edu

Dongxi Zheng, M.S.
Research Assistant
1249A Engineering Hall, 1415 Engineering Drive, Madison WI 53706
Phone: (608)335-0889
Email: dzheng3@wisc.edu

Andrea R. Bill
Associate Researcher
B243 Engineering Hall, 1415 Engineering Drive, Madison, WI 53706
Phone: (608)890-3425, Fax: (608)262-5199
Email: bill@wisc.edu

David A. Noyce, Ph.D. PE
Professor
Director, Traffic Operations and Safety (TOPS) Laboratory
1204 Engineering Hall, 1415 Engineering Drive, Madison, WI53706
Phone: (608)265-1882, Fax: (608)262-5199
Email: noyce@engr.wisc.edu

Traffic Operations and Safety (TOPS) Laboratory
Department of Civil and Environment Engineering
University of Wisconsin-Madison

5237 + 2 Table ×250 +7 Figures×250 = 7487 words (Revised 11/15/2012)

1 **ABSTRACT**

2 Autonomous vehicles are attracting more and more attention as a promising approach to improve
3 both highway safety and efficiency. Most previous studies on autonomous intersection
4 management relied heavily on custom-built simulation tools to implement and evaluate their
5 control algorithms. The use of the non-standard simulation platforms makes comparison between
6 different systems almost impossible. Additionally, without support from standard simulation
7 platforms, reliable and trustworthy simulation results are hard to obtain. In this context, this
8 paper explores a way to model autonomous intersections using VISSIM, a standard microscopic
9 simulation platform. Specifically, a reservation-based intersection control system, named
10 Autonomous Control of Urban TrAffic (ACUTA), was introduced and implemented in VISSIM
11 using VISSIM's External Driver Model. The operational and safety performances of ACUTA
12 were evaluated using the easy-to-use evaluation tools of VISSIM. Compared with the optimized
13 signalized control, significantly reduced delays were resulted from ACUTA along with a higher
14 intersection capacity and lower volume-to-capacity (v/c) ratios under various traffic demand
15 conditions. The safety performance of ACUTA was evaluated using the Surrogate Safety
16 Measure Model, and presented few conflicts among vehicles within the intersection. Moreover,
17 the key steps and elements for implementing ACUTA in VISSIM are introduced in the paper,
18 which can be useful for other researchers and practitioners in implementing their autonomous
19 intersection control algorithms in a standard simulation platform. By using a standard simulation
20 platform, performance of different autonomous intersection control algorithms can be eventually
21 compared.

22
23
24
25
26
27
28
29
30
31
32
33
34
35
36
37
38
39

40 INTRODUCTION

41 With the rapid advances in sensing, information processing, machine learning, control theory and
42 automotive technology, wide application of autonomous vehicles on highway systems is no
43 longer a dream, but a reality in near future. Autonomous vehicles are vehicles without human
44 intervention (in-vehicle or remote) and are capable of driving in real-world highway systems by
45 performing complex tasks such as merging, weaving, and driving through intersections. Many
46 automotive manufacturers including General Motors, Ford, Mercedes-Benz, Volkswagen, Audi,
47 BMW, Volvo, and Cadillac have already begun testing their autonomous vehicle on highway
48 systems (1). Google is also developing and testing its Google driverless car. As of 2012, Florida,
49 Hawaii, Nevada, Oklahoma, and California have legalized or are considering legalization of
50 autonomous cars (1). All these facts indicate that the autonomous vehicles are set to appear on
51 road in near future.

52 Most field tests for autonomous vehicles were restricted to highway segment testing.
53 Intersection control of autonomous vehicles has been studied by researchers (2-19), however,
54 implementation in practice is difficult because intersections create more conflict points than
55 highway segments. For example, when vehicles arrive at an intersection from different
56 approaches, the right of way for traversing the intersection needs to be determined. Traditional
57 intersections use traffic control devices, such as stop signs and traffic signals, to regulate vehicles
58 right of way. For managing autonomous vehicles at intersections, the right of way may be
59 controlled by an intersection central controller through vehicle-infrastructure (V2I)
60 communications (2-12), or through negotiation between vehicles via vehicle-vehicle (V2V)
61 communications (13-17).

62 Studies have been conducted to explore ideas and algorithms for managing autonomous
63 vehicles at intersections. By control strategy, the autonomous intersection control can be
64 classified into centralized control and decentralized control. For centralized control, all vehicles
65 establish communication connections to an intersection central controller, or intersection
66 manager (2-12). The intersection manager determines the vehicles' passing sequence. In a
67 decentralized control system there is no intersection manager. The passing sequence is typically
68 negotiated by vehicles based on a certain protocol (13-17). Among all these available solutions,
69 the reservation-based centralized control system has been found to work best for urban
70 intersections with high traffic demand because of its mechanism of maximizing the intersection
71 capacity (14).

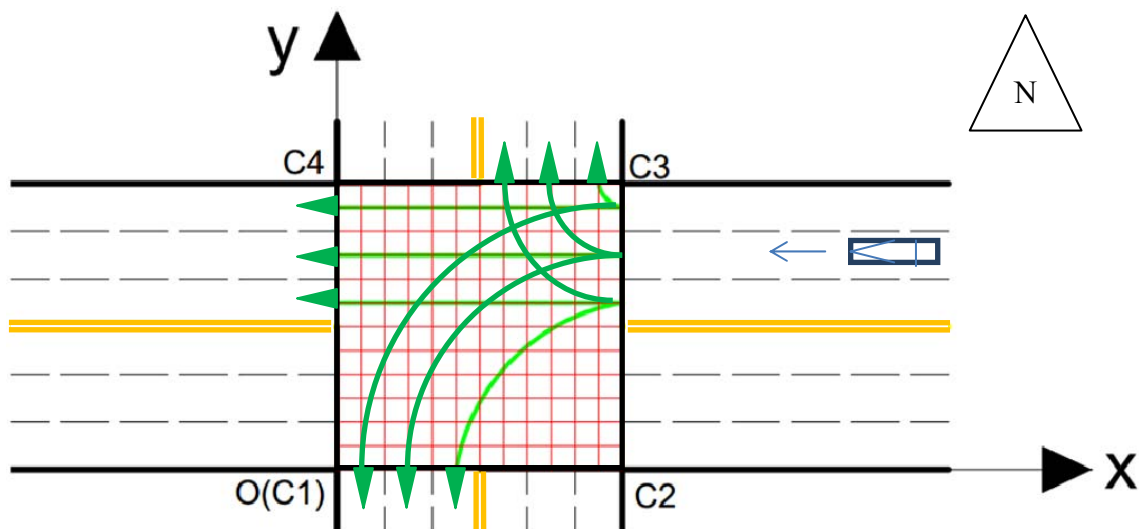
72 Due to the complexity of field implementation, most researchers used traffic simulation
73 to validate their developed strategies for autonomous intersection control. However, none of the
74 exiting studies used standard commercial traffic simulation software such as VISSIM or
75 CORSIM when evaluating the performance of their proposed strategies. Rather, simulation tools
76 developed by the respective authors were used in the evaluation process, which made the results
77 less reliable and hard compare with each other. In addition, it was noticed that most existing
78 studies lacked standard usage of terms and clear description of simulation parameter settings
79 when presenting the evaluation results. For example, when presenting the traffic volume, no
80 clarification of whether the volume is per lane or per entire approach was presented. Also, terms
81 to define lane configurations, speed distribution, volume, and delay, as well as the number of
82 runs per experiment, random seed selection, and simulation period were excluded from the
83 analyses, or were not consistently defined across different studies. Most likely the inconsistency
84 is due to the usage of different custom-built simulation software programs, rather than standard
85 commercial simulation software packages.

86 Standard simulation packages like VISSIM and CORSIM can provide standard parameter
 87 settings and outputs. In addition, using the standard package can guarantee reliable vehicle
 88 generation, car-following, lane-changing, and many other driving behavior related modeling in
 89 the simulation. Flexible settings of speed distribution, heavy vehicle percentage, and
 90 distributions of acceleration and deceleration rates can also be simply achieved, along with
 91 strong evaluation outputs like travel time and delay. Moreover, commercial packages like
 92 VISSIM have options to output vehicle trajectories, which can be directly imported into
 93 Surrogate Safety Assessment Model (SSAM) to analyze the safety performance of the
 94 intersection (19).

95 Wu et al. indicated in their paper that they chose to develop their own simulation tool
 96 rather than use standard traffic simulation packages such as VISSIM, AIMSUN, or PARAMICS,
 97 because the standard packages do not allow vehicles to be controlled individually (14). In fact,
 98 VISSIM offers flexible customization functions to facilitate building different special
 99 applications through APIs and COM extensions. All these functions offer the potential to
 100 implement applications for autonomous intersection control. In this paper, implementation of a
 101 reservation-based system in VISSIM using VISSIM's External Driver Model is presented. The
 102 establishment of the simulation model, implementation of the reservation-based control
 103 algorithm, and finally evaluations of operational and safety performance are discussed.

105 ENHANCED RESERVATION-BASED AUTONOMOUS INTERSECTION CONTROL

106 A reservation-based system utilizes a centralized control strategy for managing fully-autonomous
 107 vehicles at an intersection. All vehicles in a reservation-based system communicate only to a
 108 centralized intersection controller, namely, intersection manager (IM). The IM regulates the
 109 intersection by determining the passing sequence of all the approaching vehicles (2-10).



111
 112
 113 **FIGURE 1 Intersection mesh of tiles and example of vehicle's possible routing decisions.**
 114

115 The system presented in this paper is named as Autonomous Control of Urban Traffic
 116 (ACUTA), which is developed based on First-Come-First-Serve (FCFS) reservation-based
 117 protocol (2) with enhancements to improve some operational issues identified in previous studies
 118 (2, 8). These issues include the "starvation" issue where approaching vehicles on the side street

119 cannot get reservations when the traffic demands on the major and side street are unbalanced;
 120 and (2) slow-speed reservation issue which unnecessarily occupies many intersection resources.
 121 ACUTA regulates an intersection which is divided into a mesh of n by n tiles, as shown in Figure
 122 1, where n is termed as granularity, and reflects the tile density of the intersection mesh.

123 In ACUTA, each approaching vehicle sets up a communication connection with the IM
 124 after it enters the IM's communication range. When connected, the vehicle immediately sends
 125 the IM a reservation request along with the vehicle's location, speed and routing information (i.e.,
 126 making a left/right turn or going straight), indicating its intention to traverse the intersection. The
 127 IM processes the reservation request by computing the required time-spaces for the vehicle to get
 128 through the intersection (i.e., intersection tiles that will be occupied by the requesting vehicle for
 129 all simulation steps when the vehicle traverses the intersection) based on the location, speed,
 130 maximum acceleration rate, and the routing information provided by the requesting vehicle.
 131 Acceleration from the requesting vehicle's current location to the entrance boundary of the
 132 intersection is considered when computing the required time-spaces. Using different acceleration
 133 rates can change the required time-spaces significantly. The alternative acceleration rate shall fall
 134 within the range from zero to the maximum acceleration rate of the particular vehicle, and is
 135 calculated using the following equation.

$$a_i = 0 \quad (i = 1)$$

$$a_i = a_{\max} - (i - 1) \frac{1}{m} a_{\max} \quad (i > 1) \quad (1)$$

136
 137 Where, α_i = i^{th} alternative acceleration rate (ft/s²);
 138 α_{\max} = maximum acceleration rate (ft/s²); and,
 139 m = maximum number of internal simulations.

140 The maximum acceleration rate is one of the characteristics particularly pertaining to the
 141 requesting vehicle. However, the vehicle must maintain a constant speed when traversing the
 142 intersection. In other words, after the vehicle's center point enters the intersection, the vehicle
 143 speed does not change until the vehicle completely clears the intersection. The IM checks
 144 whether the required intersection tiles have already been reserved by other vehicles at every
 145 simulation step. If a conflict is detected, an alternative acceleration rate will be used to compute
 146 the required time-spaces, and conflicts will be checked again based on the updated required time-
 147 spaces. This iterative process is called internal simulation. The maximum number of trials of the
 148 alternative acceleration rates is termed as the maximum number of internal simulations
 149 (MAXNIS). If all alternative acceleration rates are tried out in the internal simulation and
 150 conflicts in reservation still exist, the reservation request will be rejected; otherwise, the
 151 reservation request will be approved by the IM. The IM automatically rejects the requests from a
 152 vehicle following a vehicle that is without a reservation.

153 After making a decision to reject a reservation request, the IM sends a rejection message
 154 to the requesting vehicle with a designated deceleration rate, which can be calculated using the
 155 following equation.

$$a_{Dec} = \frac{v_0^2}{2(s_0 - d_0 - v_0 \delta)} \quad (2)$$

157 Where, α_{Dec} = designated deceleration rate (ft/s²);
 158 v_0 = vehicle's speed at the time when submitting the request (ft/s);
 159 S_0 = vehicle's distance from intersection at the time when submitting request (ft);

160 δ = vehicle response time (s); and,
161 d_0 = distance from the intersection to the advance stop location (ft).

162 Vehicle response time (δ) in Equation (2) is the time interval between the instant when a
163 vehicle receives a rejection message from the IM and the instant the vehicle applies the
164 deceleration rate. Variable ' δ ' is analogous to the driver's perception reaction time in human-
165 operating vehicles. In ACUTA, the default δ is zero, which assumes ideal condition with
166 negligible response time. This assumption is based on the research findings that the DSRC
167 (Dedicated Short Range Communications), which is widely used in the Connected Vehicles
168 research, can achieve negligible delays in milliseconds for transmitting messages and activating
169 in-vehicle safety applications (20, 21). For the simplicity of modeling, the milliseconds delay is
170 assumed as zero in the current version of ACUTA. The advance stop location (ASL) (d_0) in
171 Equation (2) is a special parameter in ACUTA, which designates a predefined advance stop
172 location other than the traditional stop line close to the intersection for vehicles with rejected
173 reservation. The ASL is introduced in ACUTA as a major enhancement strategy to address the
174 slow-reservation-speed issue pertaining to vehicles stopping at the traditional stop line. By using
175 the ASL, vehicles with rejected reservations can stop at an upstream distance from the entrance
176 of the intersection; hence gain higher speed when reaching the entrance point of the intersection.
177 A higher entrance speed can increase the chance for the vehicle to get a reservation, meanwhile
178 saving the intersection time-space resources by reducing the vehicle's total traversal time within
179 the intersection. A vehicle with a rejected reservation request will apply the designated
180 deceleration rate and start to decelerate as soon as the rejection message is received. The vehicle
181 keeps sending reservation requests until the request is finally approved by the IM.

182 If the IM approves a reservation request, it sends an approval message to the requesting
183 vehicle along with a designated acceleration rate that will result in no conflicts with existing
184 reservations. Timestamps indicating when to end the acceleration and when to completely clear
185 the intersection are also sent to the vehicle in the approval message. The approved vehicle will
186 follow the acceleration instruction as soon as it receives the approval message until the vehicle
187 completely clears the intersection.

188
189

190 **MODELING ACUTA IN VISSIM**

191 Implementation of ACUTA in VISSIM is realized in this research. In this section how ACUTA
192 algorithm is modeled in VISSIM is presented. The establishment of the simulation model, the
193 algorithm for determining occupied intersection tiles, and implementation of ACUTA using
194 VISSIM external driver model are elaborated in this section.

195

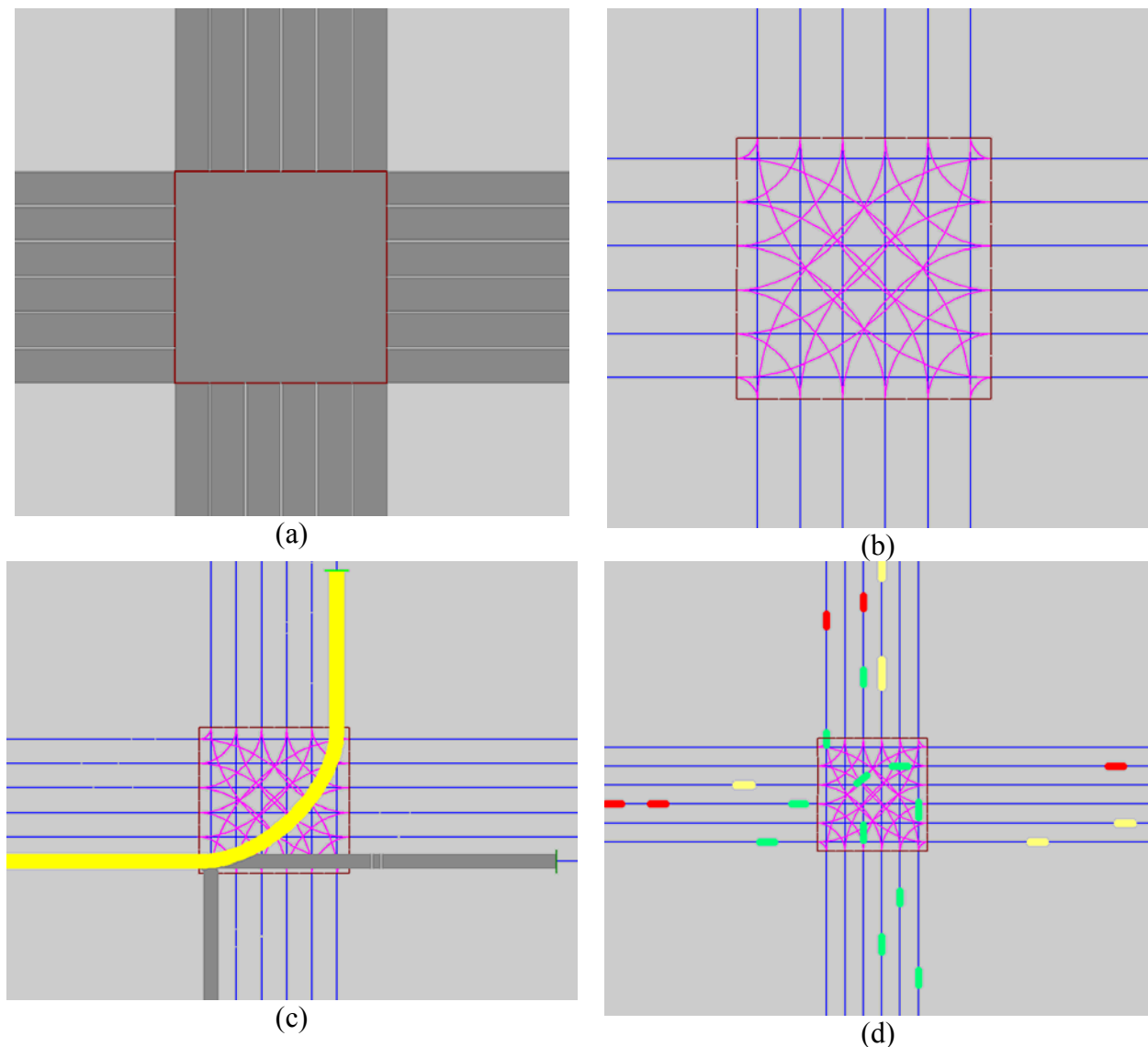
196 **Simulation Model of ACUTA Intersection**

197 ACUTA was modeled at a four-legged intersection with three lanes per direction, as shown in
198 Figure 2.a. Different from traditional signalized intersections, vehicles can turn from any lanes in
199 an ACUTA intersection, (shown in Figure 2.b) to eliminate en-route lane changes required for
200 turning vehicles, which are a significant contributing factor to vehicle delays due to conflicts
201 caused by vehicle lane change maneuvers.

202 Each approach of the intersection is more than 2000 feet long with a fixed lane width of
203 12 feet. The input traffic volume of each lane is identical to create balanced traffic demands from
204 all lanes of the intersection. Each lane has three routing decisions: left turn, through, and right
205 turn. The volume assignments to the routing decisions are the same for all lanes, namely 25%

206 for left turn, 60% for through, and 15% for right turn. Figure 2.c illustrates the routing decisions
 207 of a particular lane. Vehicle composition used is 93% passenger cars and 7% heavy vehicles. The
 208 speed distribution of traffic is also fixed at a setting equivalent to the 30 mph speed limit. These
 209 settings of VISSIM parameters like approach length, volume distribution, heavy vehicle
 210 percentage, made it a unique case of simulation. VISSIM provides simple options to change its
 211 parameter configurations including all of the aforementioned settings. Different settings are not
 212 expected to make ACUTA more complicated.

213 No priority rules, conflict areas, desired speed decisions, reduced speed areas, traffic
 214 signals, or stop signs are used in the simulation model, because the traffic control at the
 215 intersection is governed by the intersection manager only. Figure 2.d illustrates the screenshot of
 216 a simulation run, in which the red vehicles are vehicles that do not have a reservation; green
 217 vehicles are vehicles that have a reservation and are in the process of passing the intersection;
 218 and, yellow vehicles are those that have already cleared the intersection.



219 **FIGURE 2 Simulation model of the ACUTA intersection.**
 220

219
 220

221 **Implementation of ACUTA using VISSIM's External Driver Model**

222 Before the VISSIM External Driver Model (EDM) was selected for implementing ACUTA,
223 feasibility of using VISSIM COM Interface and VISSIM C2X API was investigated. The C2X
224 API specializes in modeling Car-Car communications with a designated communication range
225 for each vehicle. Therefore, by using the C2X API, it might not be possible to obtain information
226 from all of the vehicles, which is not appropriate for implementing centralized control strategies.
227 The COM interface is quite flexible and versatile in collecting vehicles information and
228 modifying vehicles parameters during the simulation period. However, the COM interface does
229 not provide a direct function to modify a vehicle's acceleration rate. It was also found that
230 executing a command through COM interface may take up to 0.2 sec, which is too long to assure
231 the efficiency of ACUTA simulations.

232 The VISSIM EDM, on the other hand, can meet all requirements for implementing
233 ACUTA. Through EDM, VISSIM provides an option to bypass and replace VISSIM's internal
234 driving behavior. During a simulation run, VISSIM calls the EDM DLL at every simulation step
235 to pass the current state of each vehicle to the DLL. Therefore, in this research, an intersection
236 manager class was built in the EDM DLL to collect each vehicle's speed, location, vehicle class,
237 maximum acceleration rate, length, width, and many other parameters pertaining to the particular
238 vehicle at each simulation step. The intersection manager processes all reservation requests at the
239 beginning of each simulation step, and passes its decision and the suggested
240 acceleration/deceleration rate to the vehicles in the same simulation step. The vehicle then passes
241 its acceleration/deceleration rate back to VISSIM at the same simulation step, thus the real-time
242 control of each vehicle's acceleration rate is realized.

243 In summary, EDM offers technical readiness for implementing ACUTA in VISSIM. Key
244 steps for realizing the reservation-based system are discussed in the following subsections.

245

246 *Modeling the Intersection Mesh in VISSIM*

247 In VISSIM, an intersection can be viewed as an overlapping square between the two crossing
248 roads. The entire intersection area can be divided into a mesh of n by n tiles, as shown in Figure
249 1. 'n' is the granularity of the intersection mesh. More or fewer tiles can be obtained by adjusting
250 the granularity. Using westbound direction as an example, the green lines with arrows illustrate
251 all possible vehicle paths to traverse the intersection.

252 In Figure 1, a two-dimensional coordinate system is projected on to the intersection area
253 to facilitate the computation of a vehicle's location. The origin O is located at the southwest
254 corner (C1) of the intersection. The southeast, northeast, and northwest corners are labeled by C2,
255 C3, and C4, respectively. The following sections use this coordinate system as a global
256 coordinate system for computing vehicle's location.

257

258 *Locating Vehicle's Central Point*

259 A key step in the internal simulation is to compute a vehicle's location at a given simulation time
260 step. For convenience in the following discussion, beginning of time is assumed to be the
261 moment when a vehicle's central point reaches boundary of the intersection area (i.e., at the
262 Point S in Figure 3).

263 In ACUTA, a vehicle maintains a constant speed after its central point enters and before
264 its central point clears the intersection area. Figure 3.a illustrates a case of through movement.
265 The path of a through vehicle is parallel to either of the axes (Figure 3.a) depending upon
266 whether the vehicle is going EB/WB or NB/SB. Assuming that the through vehicle's central

267 point reaches the boundary point $S(x_s, y_s)$ at time 0, the coordinates of the vehicle's central point
 268 can be calculated using the following equation.

$$\begin{cases} x_t = x_s - L \\ y_t = y_s \end{cases} \quad (3)$$

Where, x_t = x coordinate of the vehicle's central point at time t (ft);
 y_t = y coordinate of the vehicle's central point at time t (ft);
 x_s = x coordinate of the vehicle's central point at time 0 (ft);
 y_s = y coordinate of the vehicle's central point at time 0 (ft);
 L = $v \times t$ (ft);
 v = speed of the vehicle when it is in the intersection (ft/s); and,
 t = any time when the vehicle's central point is within the intersection (s).

269 For turning movements, the vehicle's path within the intersection can be modeled as arcs
 270 whose center coordinates are known (left turn shown in Figure 3.b and right turn shown in
 271 Figure 3.c, with the arc centers denoted as P). Assuming that the left-turn vehicle's central point
 272 reaches the boundary point $S(x_s, y_s)$ at time 0, the coordinates of the vehicle's central point can be
 273 calculated using the following equation.

$$\begin{cases} x_t = x_p - R \times \sin(\alpha + \beta) \\ y_t = y_p + R \times \cos(\alpha + \beta) \end{cases} \quad (4)$$

Where, x_t = x coordinate of the vehicle's central point at time t (ft);
 y_t = y coordinate of the vehicle's central point at time t (ft);
 x_p = x coordinate of the turning arc's center (ft);
 y_p = y coordinate of the turning arc's center (ft);
 R = $\sqrt{(x_p - x_s)^2 + (y_p - y_s)^2}$, the radius of the turning arc (ft);
 α = A/R , radian;
 β = $\arctan\left(\frac{|x_p - x_s|}{|y_p - y_s|}\right)$ (radian);
 x_s = x coordinate of the vehicle's central point at time 0 (ft);
 y_s = y coordinate of the vehicle's central point at time 0 (ft);
 A = $v \times t$, the arc length (ft);
 v = speed of the vehicle when it is in the intersection (ft/s); and,
 t = Any time when the vehicle's central point is within the intersection (s)

274 Similarly, assuming that the right-turn vehicle's central point reaches the boundary point
 275 $S(x_s, y_s)$ at time 0, the coordinates of the vehicle's central point can be calculated using the
 276 following equation.

$$\begin{cases} x_t = x_p - R \times \sin(\alpha + \beta) \\ y_t = y_p - R \times \cos(\alpha + \beta) \end{cases} \quad (5)$$

Where, x_t = x coordinate of the vehicle's central point at time t (ft);

y_t = y coordinate of the vehicle's central point at time t (ft);

x_p = x coordinate of the turning arc's center (ft);

y_p = y coordinate of the turning arc's center (ft);

R = $\sqrt{(x_p - x_s)^2 + (y_p - y_s)^2}$, the radius of the turning arc (ft);

α = A/R (radian);

β = $\arctan\left(\frac{|x_p - x_s|}{|y_p - y_s|}\right)$ (radian);

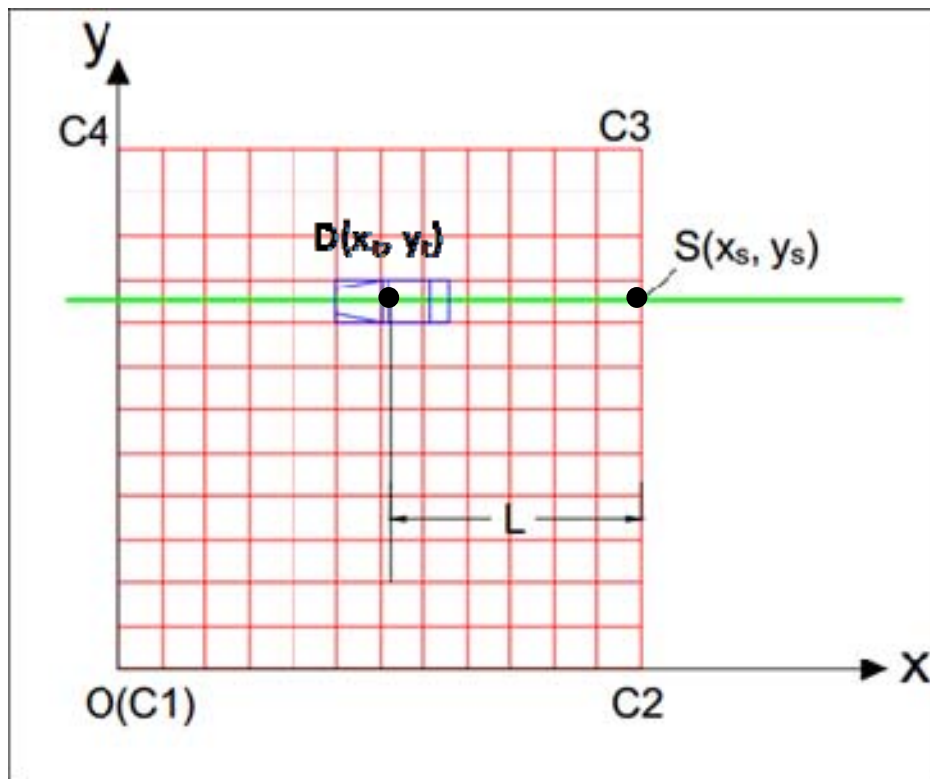
x_s = x coordinate of the vehicle's central point at time 0 (ft);

y_s = y coordinate of the vehicle's central point at time 0 (ft);

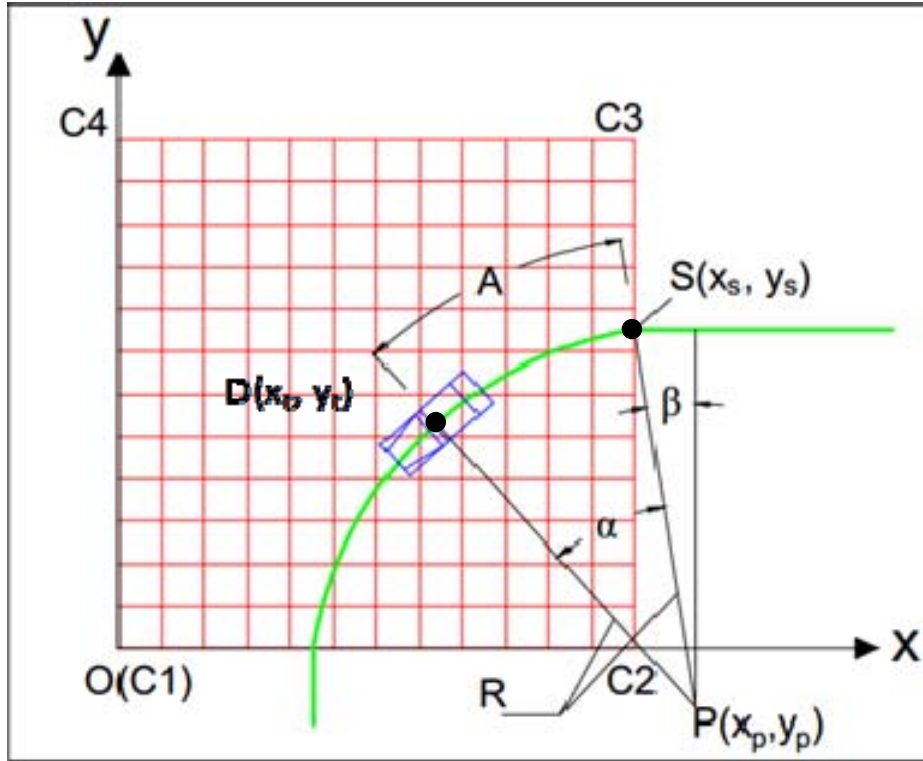
A = $v \times t$, the arc length (ft);

v = speed of the vehicle when it is in the intersection (ft/s); and,

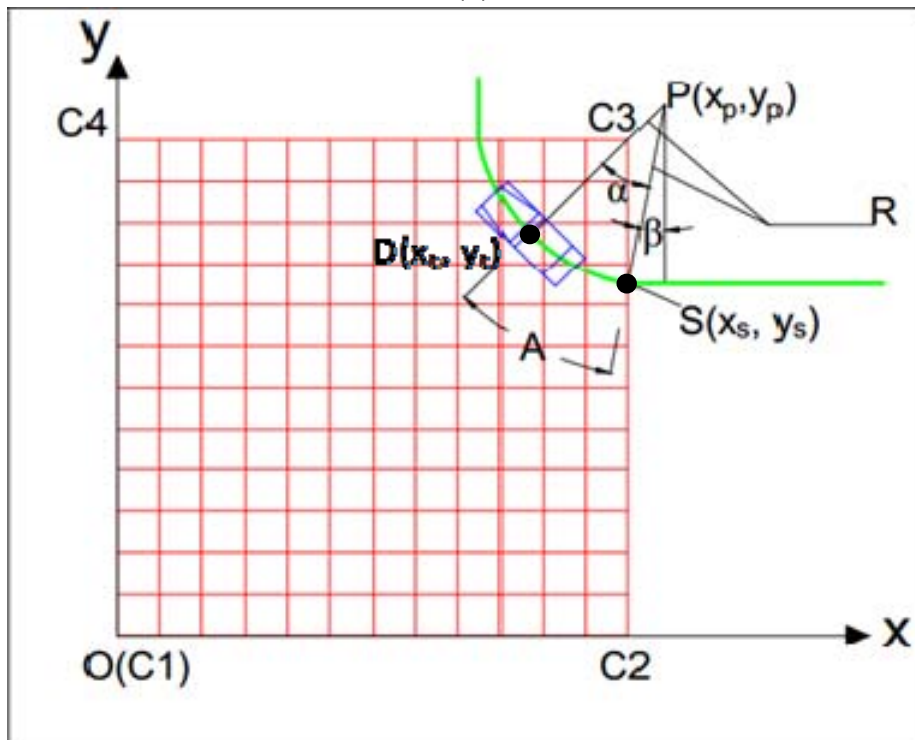
t = any time when the vehicle's central point is within the intersection (s);



(a)



(b)



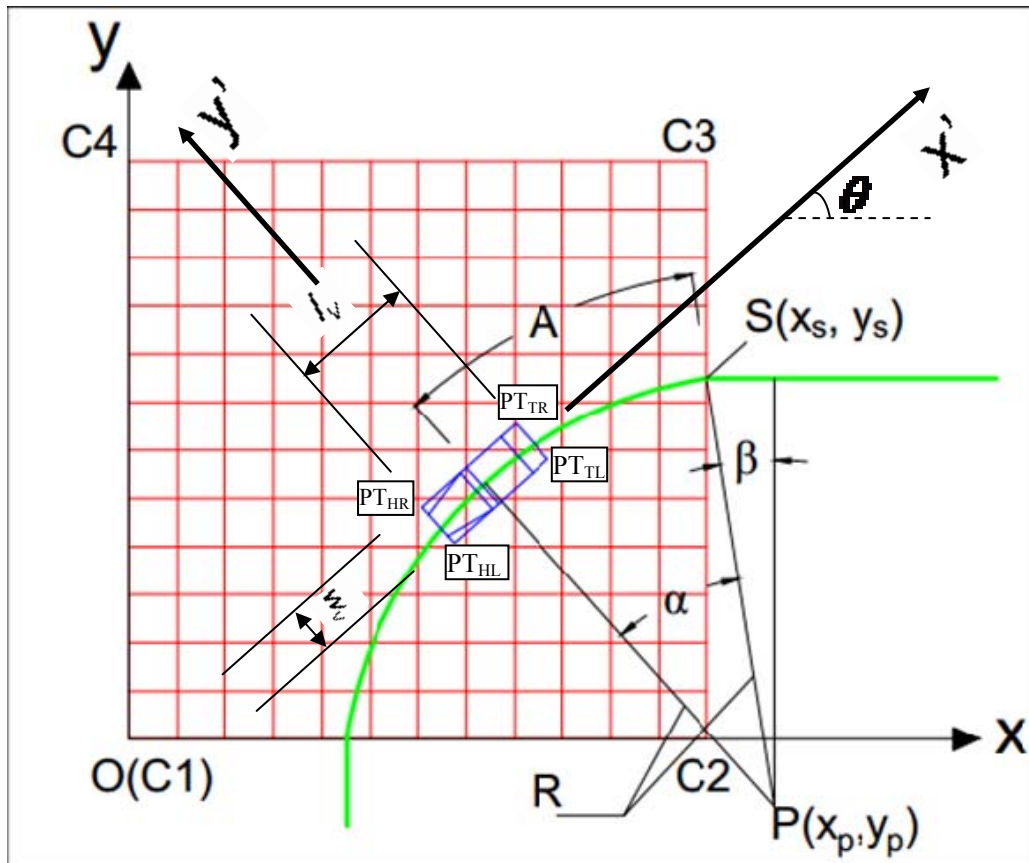
(c)

277 **FIGURE 3 Determination of vehicle central point location in intersection: (a) through**
 278 **movement; (b) left-turn; (c) right-turn.**

279 *Calculating the Coordinates of Vehicle Vertices*

280 Representing a vehicle with its central point is not adequate to describe a vehicle's location. A
 281 more comprehensive representation of a vehicle is by coordinates of the vehicle's vertices.
 282 Figure 4 illustrates the vehicle's vertices in the intersection mesh. In Figure 4, the length of the
 283 rectangle is l_v , and the width of the rectangle is w_v , equal to the corresponding vehicle's length
 284 and width, respectively. The vertices of the rectangle represents the four corners of a vehicle:
 285 head left (PT_{HL}), head right (PT_{HR}), tail left (PT_{TL}), and tail right (PT_{TR}). When the coordinates
 286 of the vehicle central point are known, they can be used to calculate coordinates of the four
 287 vertices. When the vehicle is parallel to either of the axes, coordinates of the four vertices can be
 288 easily calculated using the central point coordinates by subtracting or adding an offset of $l_v/2$ or
 289 $w_v/2$. When a vehicle is in a position shown in Figure 4, more complex coordinate transformation
 290 is needed.

291 To conduct the coordinate transformation, a local coordinate system (in comparison with
 292 the global coordinate system defined in Figure 1) needs to be defined. The origin of the local
 293 coordinate system is located at the central point of the vehicle, with the x axis pointing against
 294 the vehicle's traveling direction. To avoid confusion with the global coordinate system, an
 295 apostrophe is added to the notations of local coordinate systems (e.g., x' and y' in Figure 4).



296

297 **FIGURE 4 Determination of the coordinates of vehicle vertices.**

298 Given a point (x' , y') in the local coordinate system, its coordinates in the global system
 299 (x , y) can be calculated using a coordinate rotation followed by a coordinate transfer. The
 300 formula is given below:

$$\begin{bmatrix} x \\ y \end{bmatrix} = \begin{bmatrix} \cos \theta & -\sin \theta \\ \sin \theta & \cos \theta \end{bmatrix} \times \begin{bmatrix} x' \\ y' \end{bmatrix} + \begin{bmatrix} x_t \\ y_t \end{bmatrix} \quad (6)$$

Where, x_t = x coordinate of the vehicle's central point at time t (ft);

y_t = y coordinate of the vehicle's central point at time t (ft); and,

θ = the smallest angle measured counterclockwise from the x axis to the x' axis. In the case of Figure 1, $\theta = \alpha + \beta$ (radian).

301 Based on Equation 6, the global coordinates of the vehicle vertices can be easily
 302 converted from their local coordinates. For example, the local coordinates of the PT_{HR} vertex are
 303 ($x' = -l_v/2$, $y' = w_v/2$). By substituting x' and y' with $-l_v/2$ and $w_v/2$ in Equation 6, the global
 304 coordinates of PT_{HR} are ($x = -\frac{l_v \cdot \cos \theta + w_v \cdot \sin \theta}{2} + x_t$, $y = -\frac{l_v \cdot \sin \theta - w_v \cdot \cos \theta}{2} + y_t$).

305 *Determining Tile Occupation*

306 When coordinates of a vehicle's vertices are known, the intersection manager needs to determine
 307 which tiles are occupied by the vehicle. Figure 5 depicts a vehicle with all occupied tiles
 308 highlighted in red. The criterion to determine whether a tile is occupied by a vehicle is: at least
 309 one vertex of the tile is inside the vehicle rectangle.

310 In ACUTA, a vector based method is used to decide whether a point falls in the vehicle
 311 rectangle. As shown in Figure 5, four vectors are defined counterclockwise along the vehicle
 312 rectangle. The four vectors are \vec{v}_1 (PT_{HR}→PT_{HL}), \vec{v}_2 (PT_{HL}→PT_{TL}), \vec{v}_3 (PT_{TL}→PT_{TR}), and
 313 \vec{v}_4 (PT_{TR}→PT_{HR}). A point is within the vehicle rectangle only if it falls to the left of all the four
 314 vectors. Given a point $p(x_0, y_0)$ and a vector $\vec{v}_i [(x_{start}, y_{start}) \rightarrow (x_{end}, y_{end})]$, p falls to the left of
 315 \vec{v}_i only when the following formula is satisfied:

$$(x_0 - x_{start}) \times (y_{end} - y_0) - (x_{end} - x_0) \times (y_0 - y_{start}) < 0 \quad (7)$$

Where, x_0 = x coordinate of the testing point (ft);

y_0 = y coordinate of the testing point (ft);

x_{start} = x coordinate of the vector's start point (ft);

y_{start} = y coordinate of the vector's start point (ft);

x_{end} = x coordinate of the vector's end point (ft); and,

y_{end} = y coordinate of the vector's end point (ft);

316 On the other hand, deciding whether a vertex of a vehicle rectangle falls in a tile is
 317 relatively easy. The reason is that a tile is bounded by two horizontal lines and two vertical lines.
 318 More specifically, any point within the area of a tile can be formulated as:

$$\begin{cases} x_{low} < x_0 < x_{high} \\ y_{low} < y_0 < y_{high} \end{cases} \quad (8)$$

Where, x_0 = x coordinate of the testing point (ft);

y_0 = y coordinate of the testing point (ft);

- x_{low} = shared x coordinate of left vertices of the tile (ft);
- y_{low} = shared y coordinate of bottom vertices of the tile (ft);
- x_{high} = shared x coordinate of right vertices of the tile (ft); and,
- y_{high} = shared y coordinate of top vertices of the tile (ft);

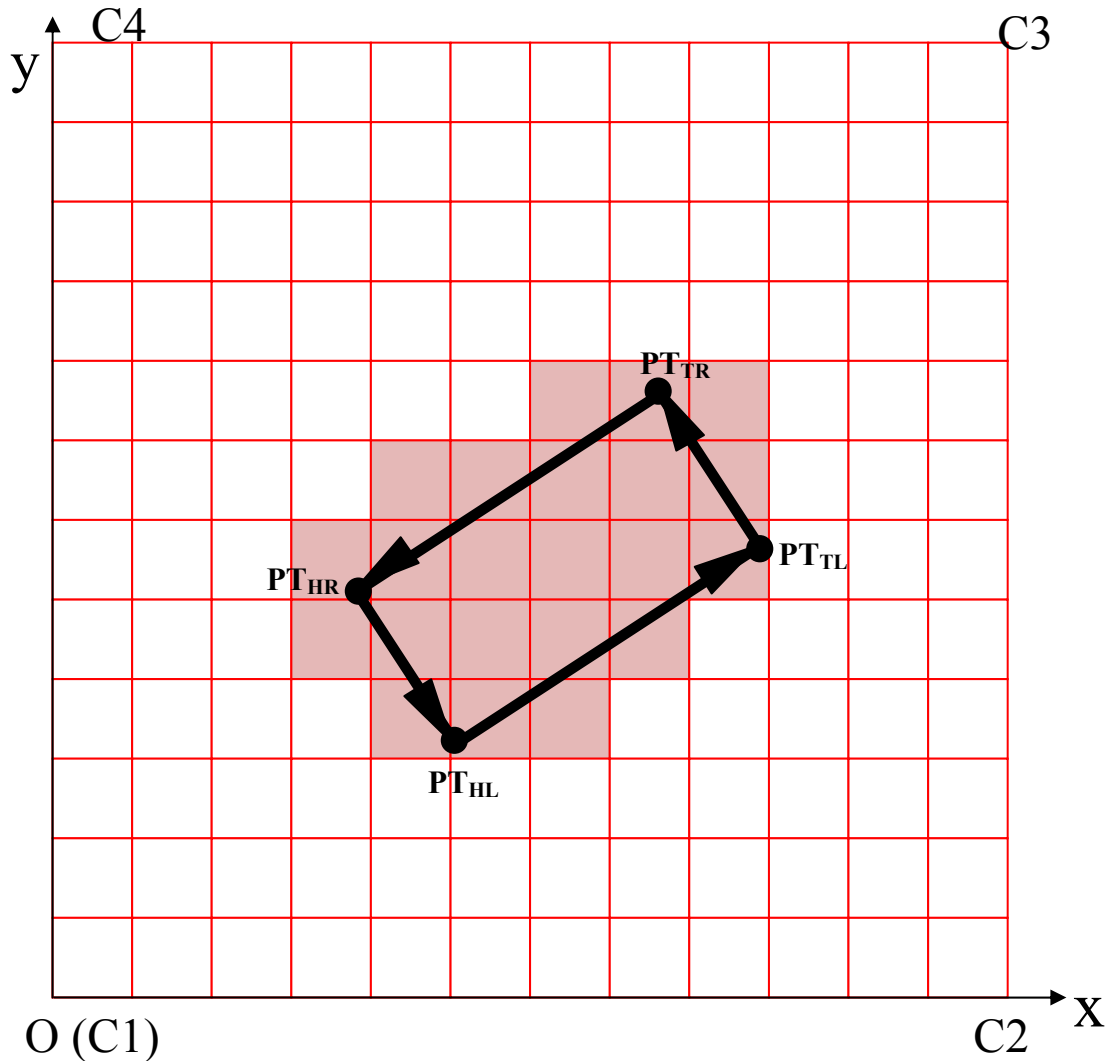


FIGURE 5 Tile occupation by a vehicle rectangle.

319
320

321

322 In summary, given a tile and a vehicle rectangle, Equations 7 and 8 are used to judge
 323 whether a vehicle rectangle has occupied a tile. If any of the four vertices of a tile satisfies
 324 Equation 7 or if any of the four vertices of a vehicle rectangle satisfies Equation 8, the tile is
 325 considered occupied by the vehicle.

326
327

328 EVALUATION OF ACUTA PERFORMANCE





329 VISSIM provides a wide range of evaluation tools for its simulation models. The section
330 discusses the evaluation for ACUTA's operational and safety performance by using VISSIM's
331 evaluation functions.

332 Operational Performance

333 ACUTA's operational performance under different traffic demand conditions was evaluated
334 using the simulation results, and was further compared with performance of a comparable
335 signalized intersection. The signalized intersection modeled in VISSIM has a left-turn lane, a
336 through lane, and a shared through and right-turn lane designated to each approach. Traffic
337 demands for each movement were identical between ACUTA model and the signalized
338 intersection model. Other parameters except lane configurations are all identical between the two
339 models.

340 For each traffic demand condition, five simulation runs with different random seeds were
341 performed. Each simulation run lasted 2,100 seconds, with the first 300 warm-up seconds
342 dropped from the evaluation. Specifically, the demand for each approach increased from 150 to
343 2850 veh/hr to cover the possible range of traffic demands. Proportions of traffic demands for
344 left turn, through and right turn movements were fixed as 25%, 60%, and 15%, respectively for
345 all the simulation runs. Specific demands by movement are summarized in Table 1. For the
346 signalized intersection model, signal timing was optimized using Highway Capacity Software
347 (22). Optimization was conducted for each tested traffic demand. Table 1 lists phasing and
348 optimized timings for the signalized intersection along with the corresponding optimized cycle
349 lengths.

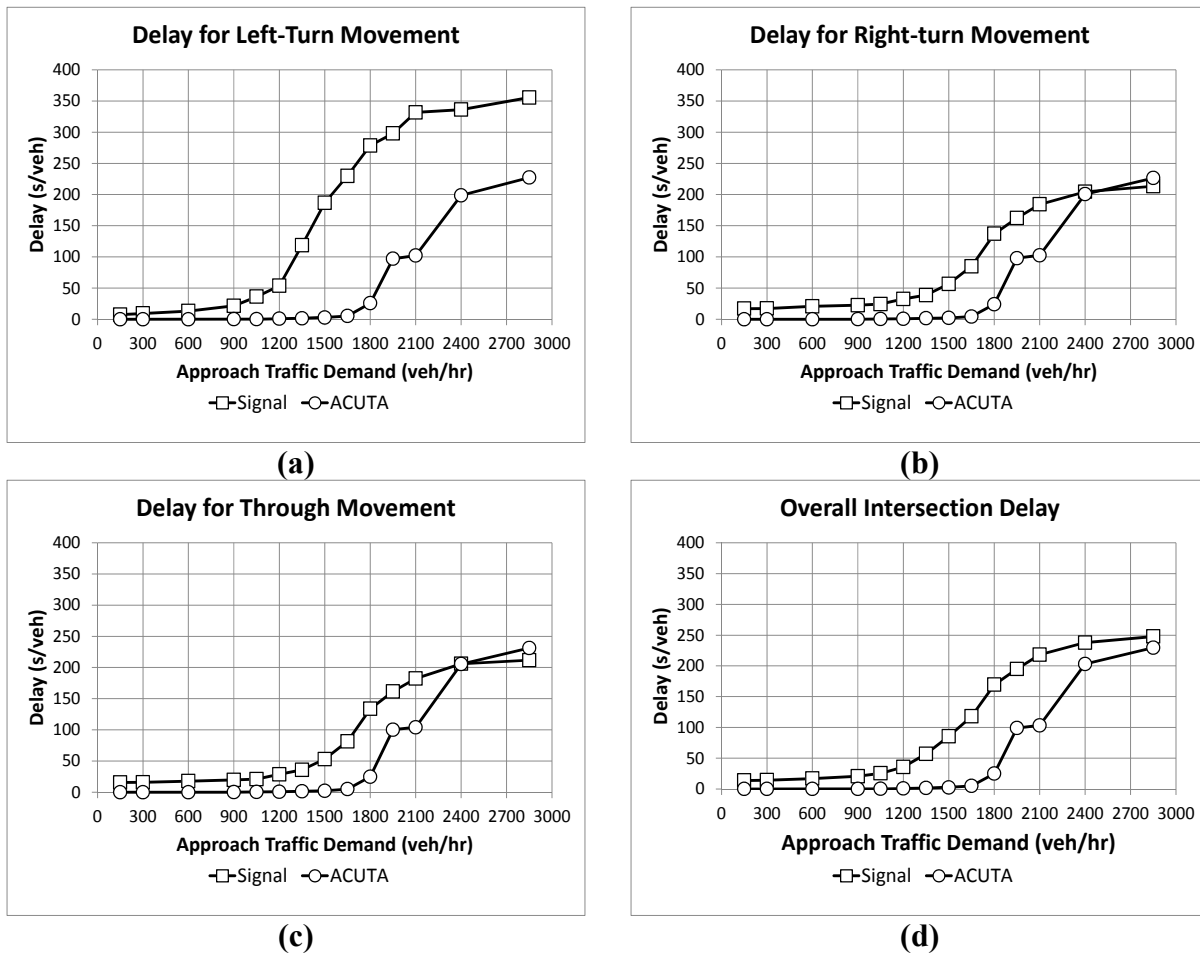
350 **TABLE 1 Traffic Demand Inputs and Optimized Timing Plan**

Approach Traffic Demand (veh/hr)	Approach Demand by Movement (veh/hr)			Signal Timing Plan				
	<i>LT</i>	<i>Thru</i>	<i>RT</i>	<i>Cycle Length (s)</i>				
150	38	90	23	40	6	6	6	6
300	75	180	45	40	6	6	6	6
600	150	360	90	60	6	16	6	16
900	225	540	135	60	6	16	6	16
1050	263	630	158	60	6	16	6	16
1200	300	720	180	90	10	28	9	27
1350	338	810	203	90	10	28	9	27
1500	375	900	225	110	12	35	12	35
1650	413	990	248	110	12	35	12	35
1800	450	1080	270	110	12	35	12	35
1950	488	1170	293	110	12	35	12	35
2100	525	1260	315	110	12	35	12	35
2400	600	1440	360	120	12	39	13	40
2850	713	1710	428	120	12	39	13	40

351 Operational performances of ACUTA and optimized signal control were assessed by
352 delays, which were obtained directly from VISSIM's output. Volume-to-capacity (v/c) ratios for
353 left turn, right turn and through movements as well as the overall intersection v/c ratio were also
354 computed for both ACUTA and optimized signal control. When computing v/c ratios, capacity (c)

355 was measured as the maximum throughput among all demand conditions, while volume (v) was
 356 directly obtained from VISSIM’s output for that specific demand condition.

357 Based on simulation results, capacities for different movements at the signalized
 358 intersection were identified to be 366 veh/hr, 218 veh/hr, and 908 veh/hr for left turn, right turn,
 359 and through movements, respectively. Capacity for an entire approach of the signalized
 360 intersection was 1480 veh/hr. Capacities for left turn, right turn, and through movements of an
 361 approach of ACUTA intersection were measured to be 501 veh/hr, 288 veh/hr, and 1185 veh/hr,
 362 respectively. Capacity for an entire approach of ACUTA intersection was 1974 veh/hr.
 363 Comparing ACUTA with signalized control, ACUTA successfully increased left turn, right turn
 364 and through capacities by 37%, 32%, and 31%, respectively. The overall approach capacity was
 365 increased by 33% by implementing ACUTA.



366 **FIGURE 6 Operational performance of ACUTA with comparison with signalized**
 367 **intersection: (a) left-turn delay, (b) right-turn delay, (c) through delay, and (d)**
 368 **overall intersection delay**

369
 370
 371

372 **TABLE 2 Comparison of Operational Performances between ACUTA and Optimized Signalized Intersection**

Approach Traffic Demand (veh/hr)	Optimized Signalized Control								ACUTA (default setting)							
	v/c ratio				Delay (s/veh)				v/c ratio				Delay (s/veh)			
	<i>LT</i>	<i>Thru</i>	<i>RT</i>	<i>Overall</i>	<i>LT</i>	<i>Thru</i>	<i>RT</i>	<i>Overall</i>	<i>LT</i>	<i>Thru</i>	<i>RT</i>	<i>Overall</i>	<i>LT</i>	<i>Thru</i>	<i>RT</i>	<i>Overall</i>
150	0.10	0.10	0.10	0.10	7.36	15.54	17.06	13.70	0.07	0.07	0.07	0.07	0.00	0.00	0.00	0.00
300	0.22	0.19	0.20	0.20	9.26	15.90	17.26	14.34	0.12	0.12	0.12	0.12	0.00	0.00	0.00	0.00
600	0.45	0.39	0.39	0.40	13.12	17.72	20.74	16.90	0.31	0.28	0.31	0.29	0.00	0.00	0.00	0.00
900	0.65	0.59	0.59	0.61	21.52	19.74	22.48	20.62	0.49	0.43	0.45	0.45	0.04	0.04	0.06	0.02
1050	0.75	0.69	0.69	0.71	36.24	21.04	24.38	25.48	0.55	0.51	0.53	0.52	0.26	0.42	0.44	0.38
1200	0.84	0.79	0.79	0.81	53.62	28.70	32.56	35.66	0.62	0.59	0.61	0.60	0.98	0.70	0.76	0.78
1350	0.90	0.88	0.89	0.89	118.72	35.82	38.68	56.86	0.70	0.67	0.67	0.68	1.46	1.48	1.64	1.50
1500	0.92	0.96	0.95	0.96	186.70	53.02	56.64	85.44	0.77	0.76	0.74	0.76	2.82	2.30	2.14	2.42
1650	0.97	0.98	0.99	0.99	230.04	81.46	84.82	117.90	0.84	0.83	0.83	0.83	5.16	4.98	4.32	4.94
1800	0.98	0.98	0.98	0.99	278.72	133.74	137.08	169.42	0.90	0.90	0.87	0.89	25.70	24.78	24.12	24.90
1950	0.98	0.99	0.98	0.99	298.04	161.54	162.30	194.98	0.91	0.91	0.89	0.91	97.00	100.20	97.86	99.04
2100	0.97	1.00	1.00	1.00	331.78	182.34	184.22	218.32	0.99	0.99	0.98	0.99	102.20	104.04	102.52	103.34
2400	0.99	0.98	0.98	0.99	336.26	206.02	204.48	237.88	0.97	0.96	0.96	0.96	198.72	205.50	200.64	203.06
2850	1.00	0.98	0.98	0.99	355.66	211.78	213.28	247.86	1.00	1.00	1.00	1.00	227.24	231.28	226.52	229.58

373

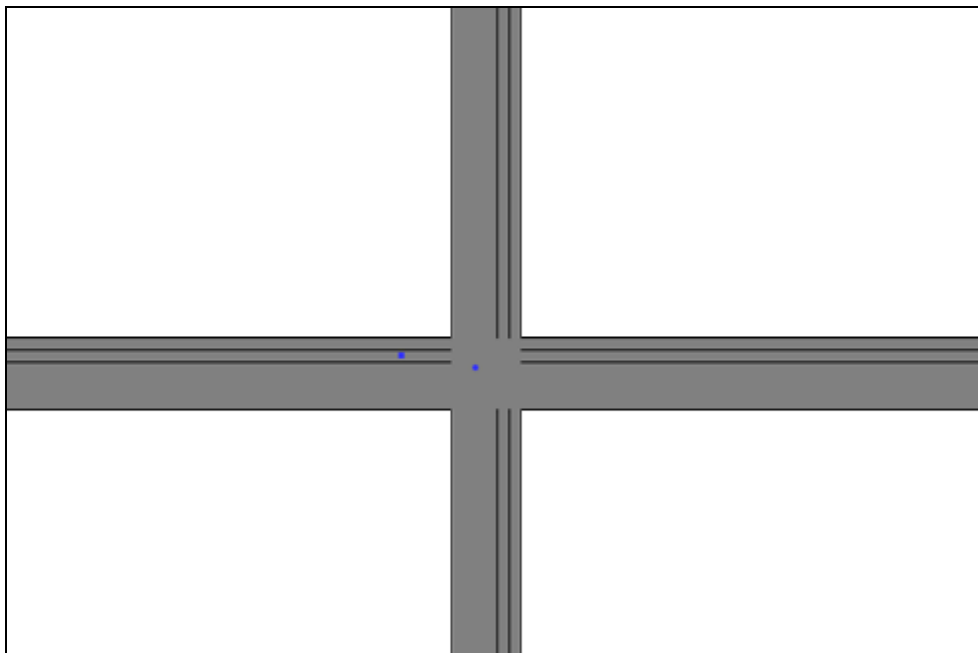
374 All evaluation results including the v/c ratios and delays are summarized in Table 2. The
375 signalized intersection reached the 0.99 overall v/c ratio when the approach traffic demand was
376 around 1650 veh/hr, while ACUTA did not reach the 0.99 overall v/c ratio until the approach
377 traffic demand reached 2100 veh/hr. These facts indicate that the ACUTA intersection can
378 process 450 extra vehicles per hour per approach without being oversaturated when compared
379 with the optimized signalized intersection.

380 Figure 6 depicts the relationships between the delays and traffic demands. Figures 6.a
381 through 6.c illustrate the delays for left turn, right turn, and through movements, respectively.
382 These figures indicate that operational performance of different traffic movements in ACUTA
383 was very balanced as delays for left-turn, right-turn, and through movements were similar under
384 all traffic demand conditions. Overall intersection delay shown in Figure 6.d was computed by
385 taking weighted average of delays for all the movements. According to Figure 6.d, overall
386 intersection delay for ACUTA remained at an extremely low level (under 5 s/veh) when
387 approach traffic demand was less than 1650 veh/hr, while signalized intersection already started
388 to operate at near capacity conditions when approach traffic demand reached 1350 veh/hr. Delay
389 for ACUTA started to increase rapidly when traffic demand reached 1800 veh/hr. However,
390 delays were still significantly less than delays for signalized intersection for approach traffic
391 demands greater than 1800 veh/hr and less than 2100 veh/hr. The superiority of ACUTA became
392 marginal at extremely high approach traffic demands of 2400 and 2850 veh/hr.

393

394 **Safety Performance**

395 VISSIM can output vehicle's trajectories, which can be directly imported into SSAM to analyze
396 traffic conflicts, enabling evaluation of safety performance of ACUTA. The result of a safety
397 performance study of ACUTA using SSAM is shown in Figure 7, which illustrates an example
398 of a conflict map obtained from SSAM. Only one traffic conflict was found within the
399 intersection during a simulation run of 1800 simulation seconds. This conflict could have been
400 eliminated by incorporating safety buffer, which will be done in the next phase of this study.



401

402

FIGURE 7 Conflict map from SSAM

403 CONCLUSIONS

404 A major contribution of this research is the successful implementation of a reservation-based
405 autonomous intersection system in a standard simulation platform, VISSIM. Feasibility of using
406 VISSIM's External Driver Model for modeling autonomous vehicle operations at a centralized
407 controlled intersection through V2I communications has been demonstrated. This type of
408 implementation has not been realized before or even been discussed in literatures. Particularly,
409 key steps for implementing ACUTA in VISSIM are introduced in this paper, providing
410 references to other researchers who are interested in implementing autonomous intersections in a
411 standard simulation platform. By using standard simulation platform, simulation results can
412 become more reliable and trustworthy. Most importantly, operational performance of different
413 autonomous intersection control algorithms can be eventually compared to each other under the
414 same simulation platform.

415 Evaluation results obtained from VISSIM demonstrated that ACUTA operated with a
416 high efficiency (i.e. intersection delay < 5 s/veh) when the approach traffic demand was less than
417 1650 veh/hr. In addition, ACUTA had balanced delay distributions for left-turn, right-turn, and
418 through movements than under all traffic demand conditions. Comparing ACUTA with the
419 optimized signal control, ACUTA successfully increased left turn, right turn and through
420 capacities by 37%, 32%, and 31%, respectively. The overall approach capacity was increased by
421 33% by implementing ACUTA. The analysis on the v/c ratios indicates that the ACUTA
422 intersection could process 450 extra vehicles per hour per approach without being oversaturated
423 when compared with the optimized signalized intersection. Finally, the safety assessment
424 showed only one conflict during a simulation run. All these findings indicate that ACUTA was
425 well modeled in the VISSIM environment. .

426

427 ACKNOWLEDGEMENT

428 The research presented in this paper was funded by the National Center for Freight &
429 Infrastructure Research and Education (CFIRE) at the University of Wisconsin-Madison.

430

431 REFERENCES

- 432 1. Autonomous Car, *Wikipedia*, http://en.wikipedia.org/wiki/Autonomous_car#cite_note-24,
433 *accessed 7/31/2012*.
- 434 2. Dresner, K. and Stone, P. (2004) "Multiagent traffic management: A reservation-based
435 intersection control mechanism." *The Third International Joint Conference on Autonomous
436 Agents and Multiagent Systems*, New York, New York, USA, July 2004, 530–537.
- 437 3. Dresner, K. and Stone, P. (2005). "Multiagent Traffic Management: An Improved
438 Intersection Control Mechanism." *The Fourth International Joint Conference on
439 Autonomous Agents and Multiagent Systems*, Utrecht, The Netherlands, July 2005, 471-477.
- 440 4. Dresner, K. and Stone, P. (2005). "Turning the Corner: Improved Intersection Control for
441 Autonomous Vehicles", *Proceedings of the 2005 IEEE Intelligent Vehicles Symposium*, Las
442 Vegas, Nevada, USA, June 2005.
- 443 5. Dresner, K. and Stone, P. (2008). "A Multiagent Approach to Autonomous Intersection
444 Management." *Journal of Artificial Intelligence Research*, 31, 591–656.
- 445 6. Dresner, K. and Stone, P. (2008). "Mitigating Catastrophic Failure at Intersections of
446 Autonomous Vehicles", *Proceedings of the Seventh International Conference on
447 Autonomous Agents and Multiagent Systems*, Estoril, Portugal, May 2008, 1393-1396.

- 448 7. Shahidi, N., Au, T.C., and Stone, P. (2011). "Batch reservations in autonomous intersection
449 management." *Proceeding of The 10th International Conference on Autonomous Agents and*
450 *Multiagent Systems - Volume 3*, Richland, SC, 2011.
- 451 8. Au, T.C., Shahidi, N., and Stone, P. (2011). "Enforcing Liveness in Autonomous Traffic
452 Management", *Proceedings of the 25th AAAI Conference of Artificial Intelligence*, 1317-
453 1322.
- 454 9. Quinlan, M., Au, T.C., Zhu, J., and Stuurca, N., and Stone, P. (2010). "Bringing Simulation to
455 Life: A Mixed Reality Autonomous Intersection." *Proceedings of 2010 IEEE/RSJ*
456 *International Conference on Intelligent Robots and Systems (IROS 2010)*, October 2010.
- 457 10. Fajardo, D., Au, T.C., Waller, S.T., Stone, P. and Yang D. (2011). "Automated Intersection
458 Control: Performance of Future Innovation Versus Current Traffic Signal Control",
459 *Transportation Research Record: Journal of the Transportation Research Board*, No. 2259,
460 223-232.
- 461 11. Wu, J., A. Abbas-Turki, and A. El Moudni. (2009) "Intersection traffic control by a novel
462 scheduling model." *IEEE/INFORMS International Conference on Service Operations,*
463 *Logistics and Informatics, 2009. SOLI '09, 2009.*
- 464 12. Yan, F. Dridi, M., and Moudni, A. E. (2009) "Autonomous Vehicle Sequencing Algorithm at
465 Isolated Intersections", *Proceedings of the 12th International IEEE Conference on Intelligent*
466 *Transportation Systems*, St. Louis, MO, USA, October 3-7, 2009.
- 467 13. Wu, J., A. Abbas-Turki, A. Corrêia and A. EL Moudni, (2007). "Discrete Intersection Signal
468 Control", *IEEE International Conference on Service Operations and Logistics, and*
469 *Informatics*, Aug. 2007.
- 470 14. Wu, J., A. Abbas-Turki, and A. El Moudni. (2010) "Contextualized Traffic Controlling At
471 Isolated Urban Intersection." *The 14th World Multi-Conference on Systemics, Cybernetics*
472 *and Informatics: WMSCI 2010*, 2010.
- 473 15. VanMiddlesworth, M., Dresner, K., and Stone, P. (2008). "Replacing the Stop Sign:
474 Unmanaged Intersection Control for Autonomous Vehicles." *Proceedings of AAMAS*
475 *Workshop on Agents in Traffic and Transportation*, Estoril, Portugal, 94–101.
- 476 16. Alonso, J., Milanés, V., Joshué, P., Onieva, E., González, C., de Pedro, T., (2011).
477 "Autonomous vehicle control systems for safe crossroads", *Transportation Research Part C*,
478 19, 1095–1110.
- 479 17. Ball, R. and Dulay, N. (2010). "Enhancing Traffic Intersection Control with Intelligent
480 Objects", *First International Workshop the Urban Internet of Things*, 2010.
- 481 18. Vasirani, M. and Ossowski, S. (2009). "Evaluating Policies for Reservation-based
482 Intersection Control." *Proceedings of the 14th Portuguese Conference on Artificial*
483 *Intelligence (EPIA'09)*, Vol. 14, 2009.
- 484 19. Surrogate Safety Assessment Model and Validation: Final Report, *FHWA-HRT-08-051*,
485 Federal Highway Administration, Washington, D.C., 2008.
- 486 20. *DSRC: The Future of Safer Driving*, U.S. Department of Transportation, Research and
487 Innovative Technology Administration. [http://www.its.dot.gov/factsheets/pdf/JPO-](http://www.its.dot.gov/factsheets/pdf/JPO-034%20DSRC%20V5.5%20F.pdf)
488 [034%20DSRC%20V5.5%20F.pdf](http://www.its.dot.gov/factsheets/pdf/JPO-034%20DSRC%20V5.5%20F.pdf) (accessed 11/14/2012)
- 489 21. Hu, B. and Gharavi, H. (2011) "A Joint Vehicle-Vehicle/Vehicle-Roadside Communication
490 Protocol for Highway Traffic Safety", *International Journal of Vehicular Technology*, 2011,
491 doi:10.1155/2011/718048
- 492 22. Highway Capacity Software 2010, McTrans, University of Florida.